

Power Spectrum of Hybrid Optical Modulated Signals Employed in Cellular Mobile Communication Systems

Mohammed M. Banat, Ibrahim Ghareeb and Mohammed Hayajneh

Department of Electrical Engineering
Jordan University of Science & Technology, Irbid, Jordan
Tel: +962 2295111 /ext. 2506, Fax: +962 2295123

ABSTRACT– The power spectral density of optical hybrid M -FSK/ N -ASK (HFAM) signals is analytically evaluated in two cases. In the first case, HFAM signal is assumed to be phase noise free. In the other case, the HFAM signal is assumed to be corrupted by phase noise. The expressions obtained for the power spectrum are implemented and plotted versus the normalized frequency fT_b , where T_b is the bit duration. This is done for a group of combinations of M and N , where $M = 2, 4, 8, 16$ is the number of FSK levels and $N = 2, 4$ is the number of ASK levels. The fractional out-of-band power containment bandwidths are obtained numerically using Matlab, and plotted against fT_b for the same combinations of M and N mentioned above.

1 Introduction

In this paper we study the spectral characteristics of a cellular mobile communication system employing optical feeder [1]. The transmitted signals are modulated using a hybrid frequency amplitude (HFAM) modulation technique. This proposed hybrid ASK/FSK modulation technique is anticipated to be both power- and bandwidth-efficient. This is due to that ASK is a bandwidth-efficient technique [2], while FSK is a power-efficient technique [3].

In HFAM, every k_s -bits of the source stream is divided into two streams. The first stream of length k_f data bits is used to set the carrier frequency to one of $M = 2^{k_f}$ values. At the same time, the other stream of data bits of length k_A is used to set the ASK level to one of $N = 2^{k_A}$ values. From a signal constellation point of view, the signal space can be seen into M sets each consisting of N signals. The signals in different sets are uncorrelated and orthogonal. The $M \times N$ signals have equal time durations and different energy levels depending on the generated ASK level. The source emits a random symbol from a set of L symbols every T_s seconds, where $L = 2^{k_A+k_f}$. The expected theoretical bandwidth for such a modulation scheme is approximately $W = M\Delta f$ [5], where Δf is the frequency separation between two adjacent tones. In each symbol interval, k_s bits are transmitted. Hence, the data rate is equal to $R_b = k_s/T_s$, where T_s is the symbol interval.

This paper is organized as follows: section 2 introduces the transmitted signal model of HFAM signals. Section 3 presents an evaluation of the correlation coefficient of HFAM signals. In section 4 the power spectral density of HFAM signals is evaluated. Section 5 outlines the bandwidth efficiency achieved by the HFAM technique. Results and comparisons are presented in section 6. Finally, conclusions are summarized in section 7.

2 Transmitted signal model

A block diagram of an HFAM modulator is shown in Fig. 1. A PAM modulator generates rectangular pulses of duration T_s and amplitudes a_n according to the k_A data bits. The M -ary FSK modulator generates FSK signals with frequencies f_m , where f_m depends on the k_f data bits. The output of PAM modulator is impressed upon the output of the M -ary FSK modulator to produce the HFAM electrical signal which finally externally modulates the laser optical source to produce the optical HFAM signals.

The frequency-amplitude modulated signal corresponding to the output of the HFAM modulator can be represented as

$$s_{nm}(t) = R \{ a_n e^{j2\pi f_m t} g(t) e^{j2\pi f_c t} \} \quad 0 \leq t \leq T_s, \\ n = 1, 2, \dots, N \text{ and } m = 1, 2, \dots, M \quad (1)$$

where $R\{ \}$ denotes the real part of the complex quantity in the brackets. In (1) $a_n = \sqrt{2E_n/T_s}$, where E_n is the energy of the generated n th ASK level. f_c is the center frequency of the optical laser source, and $g(t)$ is a rectangular pulse of unity amplitude and duration T_s . The equivalent low-pass waveform of the generated optical HFAM signals can be written as

$$u_{nm}(t) = a_n e^{j2\pi f_m t} g(t), \quad 0 \leq t \leq T_s \quad (2)$$

3 Correlation coefficient of HFAM

The complex-valued correlation coefficient of HFAM signals can be defined as

$$r = \frac{1}{2\sqrt{E_n E_l}} \int_0^{T_s} u_{nm}(t) u_{lk}^*(t) dt \quad (3)$$

Where the asterisk denotes the complex conjugate. The HFAM signals satisfy the orthogonality condition if the real part of the correlation coefficient r is zero, i.e.,

$$R\{r\} = \frac{\sin(\pi\Delta f T_s)}{\pi\Delta f T_s} \cos(\pi\Delta f T_s + \theta_d) \quad (4)$$

Where $\Delta f = f_m - f_k$ is the separation between two adjacent frequency tones and θ_d is the phase difference between two consecutive symbols. It can be shown that the orthogonality condition is met when the frequency separation is $\Delta f = k/T_s$ for any integer k . The minimum frequency separation between two adjacent tones in HFAM is $1/T_s$.

4 Power spectral density

In this section the spectral density of HFAM signals is analyzed in two cases; in the first case, the HFAM signal is assumed to be with zero linewidth laser. In the other case, the HFAM signal is assumed to be with laser linewidth not equal to zero.

4.1 Spectral density with zero linewidth laser

The HFAM transmitted signals with zero linewidth laser can be represented as

$$s(t) = R \left\{ \sum_{l=-\infty}^{\infty} a_l p(t - lT_s) \exp \left(j\pi\Delta f \sum_{k=-\infty}^{\infty} I_k q(t - kT_s) \right) \exp(j2\pi f_c t) \right\} \quad (5)$$

where f_c is the carrier frequency, and

$$I_k = \pm 1, \pm 3, \dots, \pm M - 1, \quad (6)$$

$$p(t - lT_s) = \begin{cases} 1 & lT_s \leq t \leq (l+1)T_s \\ 0 & \text{elsewhere} \end{cases}$$

and

$$q(t - kT_s) = \begin{cases} 0 & t \leq kT_s \\ t - kT_s & kT_s \leq t \leq (k+1)T_s \\ T_s & t \geq (k+1)T_s \end{cases} \quad (7)$$

The equivalent low-pass form of $s(t)$ can be written as

$$u(t) = \sum_{l=-\infty}^{\infty} a_l p(t - lT_s) \exp \left(j\pi\Delta f \sum_k I_k q(t - kT_s) \right). \quad (8)$$

The power spectral density of $s(t)$, $\phi_s(f)$, is related to the power spectral density of its equivalent low-pass form, $\phi_u(f)$, by

$$\phi_s(f) = \frac{1}{2} (\phi_u(f - f_c) + \phi_u(f + f_c)) \quad (9)$$

The autocorrelation function of $u(t)$ is defined as

$$\phi_u(t + \tau, t) = E \{ u(t + \tau) u^*(t) \} \quad (10)$$

where $E \{ \}$ denotes to ensemble averaging of the argument. From the statistical independence of $\{a_l\}$ and $\{I_k\}$ sequences,

and after a number of mathematical steps, equation (10) can be written in the following form

$$\phi_u(\tau) = \frac{1}{MT_s} \sum_{n=1, \text{odd}}^{M-1} \cos(\pi\Delta f n\tau) \sum_r \phi_{aa}(r) R_{pp}(\tau - rT_s) \quad (11)$$

where

$$\phi_{aa}(m) = \begin{cases} \sigma_a^2 + \mu_a^2 & m = 0 \\ \mu_a^2 & m \neq 0 \end{cases},$$

$$\sigma_a^2 = \frac{(N^2 - 1)\Delta_d^2}{12}, \quad (12)$$

$$\mu_a^2 = \frac{N^2\Delta_d^2}{4}, \quad (13)$$

and Δ_d is the separation between two adjacent ASK levels. Also,

$$R_{pp}(\tau) = \int_{-\infty}^{\infty} p(t + \tau) p^*(t) dt \quad (14)$$

is the time average autocorrelation function. Performing the Fourier transform of the autocorrelation function in (11) to obtain the power spectral density of $u(t)$, $\phi_u(f)$.

$$\begin{aligned} \phi_u(f) = \frac{1}{2MT_s} \left\{ \sum_{n=1, \text{odd}}^{M-1} \left(\sigma_a^2 T_s^2 \left(\frac{\sin(\pi(f - \frac{n\Delta f}{2})T_s)}{\pi(f - \frac{n\Delta f}{2})T_s} \right)^2 \right. \right. \\ \left. \left. + \left(\frac{\sin(\pi(f + \frac{n\Delta f}{2})T_s)}{\pi(f + \frac{n\Delta f}{2})T_s} \right)^2 \right) \right. \\ \left. + \mu_a^2 T_s \left(\delta(f - \frac{n\Delta f}{2}) + \delta(f + \frac{n\Delta f}{2}) \right) \right\} \quad (15) \end{aligned}$$

Equation (15) denotes the exact expression for spectral density of the HFAM signals with free phase noise.

4.2 Spectral density with laser linewidth not equal to zero

The HFAM transmitted signal with laser linewidth not equal to zero $s_p(t)$ is expressed as

$$s_p(t) = R \left\{ \sum_{l=-\infty}^{\infty} a_l p(t - lT_s) \exp \left(j\pi\Delta f \sum_{k=-\infty}^{\infty} I_k q(t - kT_s) + j\theta(t) \right) \exp(j2\pi f_c t) \right\} \quad (16)$$

where $\theta(t)$ is the laser phase noise which denotes a Wiener process with variance equal to $2\pi\beta t$ where β is laser linewidth. The equivalent low-pass signal of $s_p(t)$ is given by

$$v(t) = \sum_{l=-\infty}^{\infty} a_l p(t - lT_s) \exp \left(j\pi\Delta f \sum_k I_k q(t - kT_s) + j\theta(t) \right). \quad (17)$$

The autocorrelation function of $v(t)$ is defined as

$$\phi_v(t + \tau, t) = E \{v(t + \tau)v^*(t)\} \quad (18)$$

From the independence of $\{a_i\}$, $\{I_k\}$, and $\theta(t)$ equation (18), after a number of mathematical steps, becomes

$$\begin{aligned} \phi_v(t + \tau, t) &= \frac{1}{2} E_{\theta} \{e^{j\Delta_r \theta}\} E_a \left\{ \sum_l \sum_m a_l a_m^* p(t + \tau - lT_s) \right. \\ &\quad \left. p^*(t - mT_s) \right\} \\ &\quad \times E_I \left\{ \exp(j\pi \Delta f \left[\sum_k I_k q(t + \tau - kT_s) \right. \right. \right. \\ &\quad \left. \left. \left. - \sum_n I_n q(t - nT_s) \right] \right) \right\} \quad (19) \end{aligned}$$

Where $\Delta_r \theta$ is phase fluctuations and has a Gaussian zero-mean distribution function. Evaluation of $E \{e^{j\Delta_r \theta}\}$ is done in [6] and it is given by

$$E \{e^{j\Delta_r \theta}\} = \exp \left(-\frac{R_{sp}}{4P} (1 + \beta_c^2) \tau \right) \quad (20)$$

Where R_{sp} is the rate at which spontaneously emitted photons are added to the intercavity photon population, β_c is the linewidth enhancement factor, and P is the laser power emitted at static case. By observing (20), it can be seen that it is time independent. Then spectral density of the HFAM signal with finite laser linewidth $\phi_v(f)$ is equal to the spectral density of the HFAM signal with zero linewidth $\phi_u(f)$ convolved with the fourier transform of (20). In mathematical expressions

$$\phi_v(f) = \left(\frac{1}{\frac{R_{sp}}{4P} (1 + \beta_c^2) + j2\pi f} \right) * \phi_u(f) \quad (21)$$

with some mathematical manipulations (21) becomes

$$\begin{aligned} \phi_v(f) &= \frac{1}{2M} \left\{ \left(\sigma_a^2 T_s \left(\frac{\sin \pi f T_s}{\pi f T_s} \right)^2 + \mu_a^2 \delta(f) \right) \right. \\ &\quad \left. * \sum_{n=1, \text{odd}}^{M-1} \left(\frac{2G + j4\pi f}{G^2 - 4\pi^2 (f^2 - (\frac{n\Delta f}{2})^2) + j4\pi G f} \right) \right\} \quad (22) \end{aligned}$$

where

$$G = \frac{R_{sp}}{4P} (1 + \beta_c^2) \quad (23)$$

5 Bandwidth efficiency (BE)

In this section, the bandwidth efficiency is evaluated in the light of two measures; the first is based on minimum frequency separation, the other is based on fractional power containment bandwidth.

5.1 BE based on minimum frequency separation

In section 3 it was found that for orthogonality of HFAM waveforms, the minimum separation between two adjacent tones is $1/T_s$. Consequently, the required channel bandwidth for transmission can be approximated by

$$W = M \Delta f \quad (24)$$

However, the bit rate is given by

$$R_b = \frac{\log_2 L}{T_s} = \frac{k_A + k_f}{T_s} \quad (25)$$

Hence, for heterodyne coherent envelope detection of HFAM signals, the bandwidth efficiency is given by

$$\frac{R_b}{W} = \frac{(\log_2 M + \log_2 N)}{M} \quad (26)$$

One can see that the expression in (26) shows that as the number of orthogonal sets M increases, the bandwidth required for transmission also increases and the bandwidth efficiency decreases. If the number of keying amplitudes N increases, the bandwidth efficiency increases.

5.2 BE based on fractional power containment bandwidth

The fractional out-of-band power containment is defined as [4]

$$\mu_B = 1 - \int_{-B/2}^{B/2} \phi(f) df \quad (27)$$

Where $\phi(f)$ is the power spectral density of HFAM signal either with or without phase noise. If the fractional out-of-band power containment defined in (27) is plotted against the bandwidth normalized by the bit rate (BT_b), bandwidth efficiency can be obtained directly for a given fractional power bandwidth.

6 Results and comparisons

The power spectral density of HFAM signals without phase noise given in (15) are plotted against the normalized frequency (fT_b) in Figs. 2 and 3. This is done for the HFAM combinations $MF/2A$ and $MF/4A$, where $M = 2, 4$. Also, the power spectral density of HFAM signals with phase noise given in (22) are plotted in Figs. 4 and 5 for the same HFAM combinations mentioned above. From these figures, one can see that HFAM technique needs less bandwidth than FSK for the same bit rate. For example, let us take HFAM combination $2F/2A$ and $4F$, the width of the main lobe of the spectral density of $2F/2A$ and $4F$ (without phase noise), approximately, is $0.75/T_b$ and $1.2/T_b$, respectively.

The fractional out-of-band power containments of HFAM modulated signals obtained by substituting (15) into (27) and plotted versus normalized bandwidth BT_b in Figs. 6 and

7 for the HFAM combinations $MF/2A$ and $MF/4A$ where $M = 2, 4, 8, 16$, respectively. From these plots, it can be concluded that, for any fixed M and as the number of amplitude levels N increases, the bandwidth efficiency of HFAM is increased and the out-of-band spectral tails are reduced.

7 Conclusions

In this paper, a mathematical model of HFAM signals was presented. These signals are characterized by relative simplicity and the ability to increase the volume of a signal system. We restrict our attention to the orthogonal HFAM signal model. In this signal model, the minimum frequency separation between adjacent tones of HFAM signals required to satisfy the orthogonality condition is reduced compared to FSK signals that use the same number of tones; which denotes less bandwidth is needed for the same bit rate. This model consists of M subsets of multilevel ASK signals; the signals in each subset are orthogonal to signals in all other subsets, thereby allowing individual detection of each signal set without cross interference. This paper showed that HFAM is more bandwidth-efficient modulation technique than the conventional CPFSK. Also, it showed that for large power containment the bandwidth efficiency of HFAM is comparable to that of the conventional L -ASK.

References

- [1] Makato shibutani, Toshihito Kanai, Watani Domom, Katsumi Emura, and Junji Namiki, "Optical fiber feeder for microcellular mobile communication systems(H-015)," *IEEE Journal on Selected Areas in Comm.*, Vol. 11, pp. 1118-1126, Sept. 1993.
- [2] Ozan. K. Tonguz, Okan M. Tanrikulu, and Leonid G. Kazovsky, "Performance of coherent ASK light-wave systems with finite intermediate frequency", *IEEE Trans. Com.*, Vol. 45, No. 3, pp. 344-351, Mar. 1997.
- [3] Lori L. Jeromin and Vincent W. S. Chan, "M-ary FSK performance for coherent optical communication systems using semiconductor lasers", *IEEE Trans. Com.*, Vol. COM-34, No. 4, pp. 375-381, April 1986.
- [4] Ibrahim Ghareeb, "Bit error rate performance and power spectral density of a noncoherent hybrid frequency-phase modulation system", *IEEE J. on Select. Areas in Comm.*, Vol. 13, No. 2, pp. 276-284, February 1995.
- [5] J. G. Proakis, *Digital Communications*. New York: McGraw-Hill, 1989.
- [6] D. P. Agrwal and N. K. Dutta, *Long-Wavelength Semiconductor Lasers*, Van Nostrand Reinhold Company, New York, 1986.

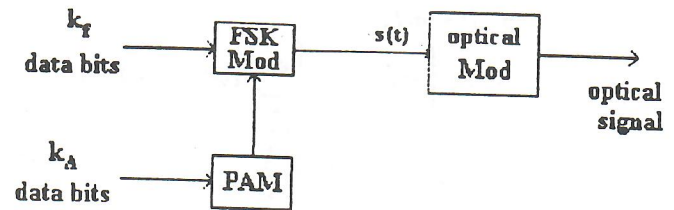


Figure 1: HFAM modulator

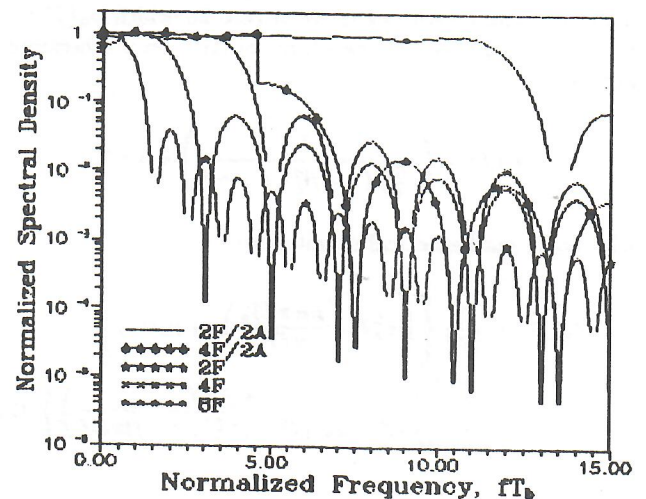


Figure 2: Normalized spectral density of the phase noise free HFAM signal and M -FSK versus the normalized frequency fT_b for $MF/2A$, $M=2,4$.

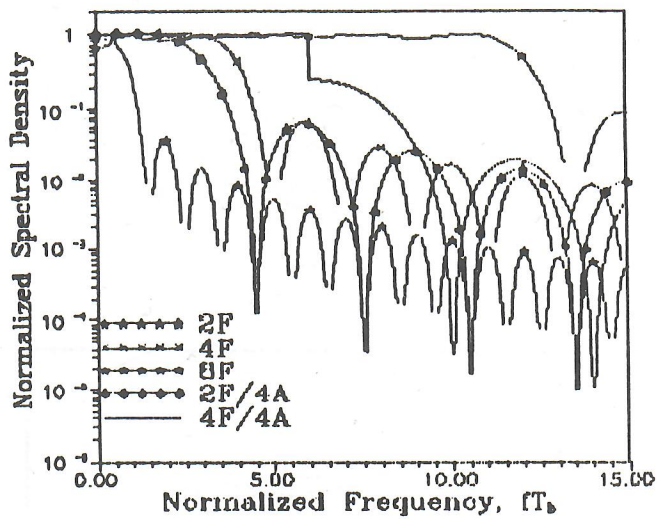


Figure 3: Normalized spectral density of the phase noise free HFAM signal and M -FSK versus the normalized frequency fT_b for $MF/4A$, $M=2,4$.

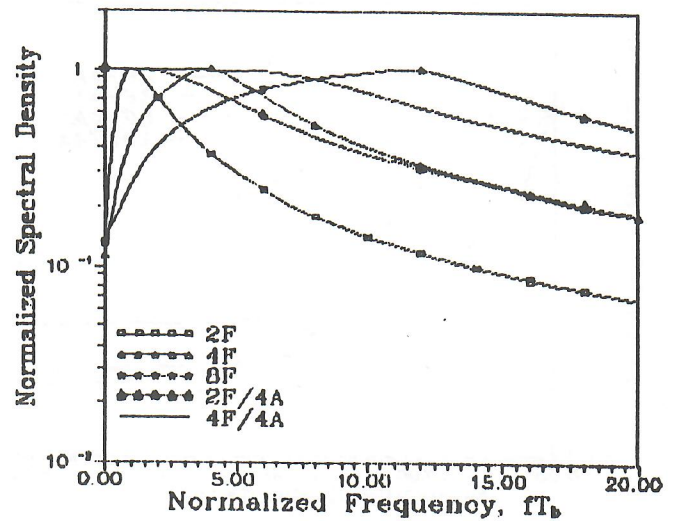


Figure 5: Normalized spectral density of the phase noise corrupted signal versus the normalized frequency fT_b for $MF/4A$ and M -FSK, $M=2,4$.

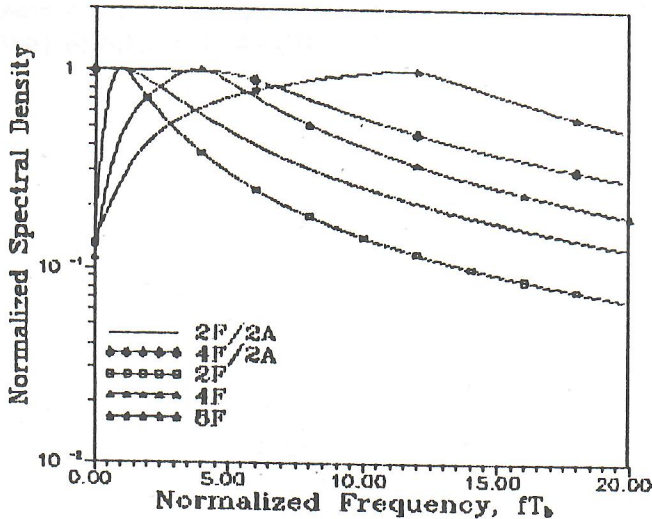


Figure 4: Normalized spectral density of the phase noise corrupted signal versus the normalized frequency fT_b for $MF/2A$ and M -FSK, $M=2,4$.

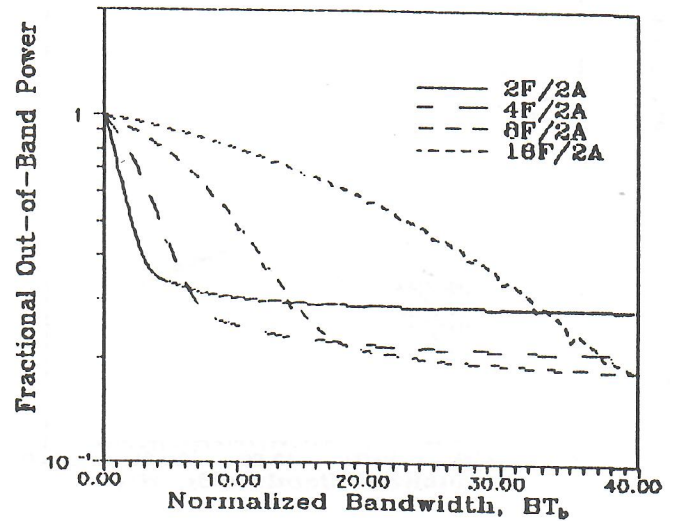


Figure 6: Fractional out-of-band power versus normalized bandwidth BT_b for $MF/2A$, $M=2,4,8,16$ (without phase noise).

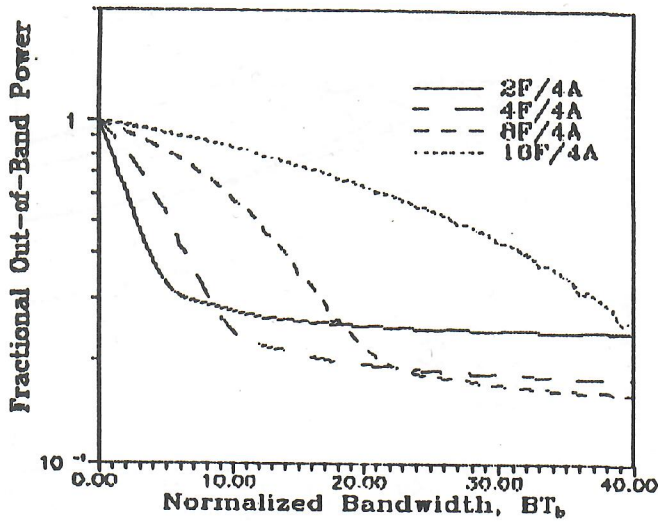


Figure 7: Fractional out-of-band power versus normalized bandwidth BT_b for MF/4A, $M=2,4,8,16$ (without phase noise).

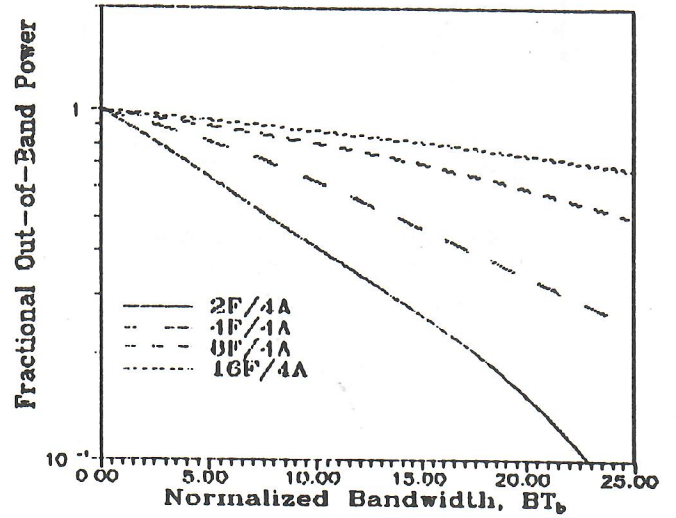


Figure 9: Fractional out-of-band power versus normalized bandwidth BT_b for MF/4A, $M=2,4,8,16$ (with phase noise).

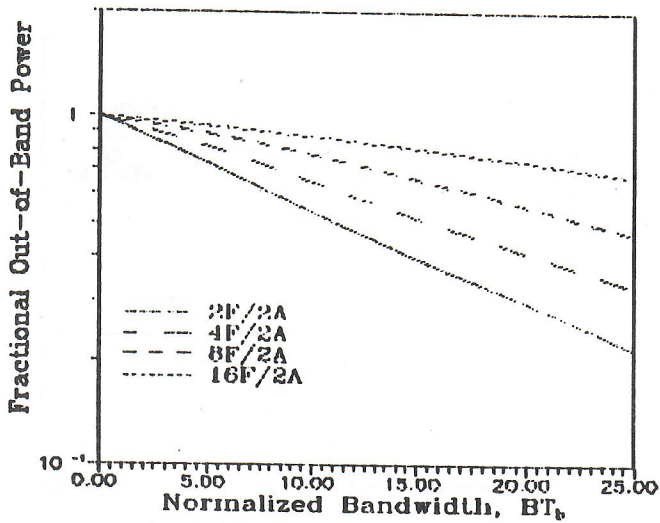


Figure 8: Fractional out-of-band power versus normalized bandwidth BT_b for MF/2A, $M=2,4,8,16$ (with phase noise).